Available online at www.sciencedirect.com

ScienceDirect

Energy Procedia 92 (2016) 764 – 772

Energy Procedia

6th International Conference on Silicon Photovoltaics, SiliconPV 2016

Simulation of spalling with a non-planar bi-layered interface due to the reuse of the substrate

Irene Berardone[a]*, Jan Hensen[b], Verena Steckenreiter[b], Sarah Kajari-Schröder[b], Marco Paggi[c]

[a]*Politecnico di Torino, Corso Duca degli Abruzzi 24, Torino 100129,Italy*
[b]*Institute for Solar Energy Research Hamelin (ISFH), Am Ohrberg 1, D-31860 Emmerthal, Germany*
[c]*IMT School for Advanced Studies Lucca, Piazza San Francesco 19, 55100 Lucca, Italy*

Abstract

Kerfless wafering techniques have the potential to reduce the cost of crystalline silicon (Si) in photovoltaics by saving material and production costs. Thermomechanical spallation from thick wafers with aluminium (Al) in the double function as stressor layer and contacting layer in the final solar cell is one attractive option. In principle this technique might allow to produce multiple thin film solar cells via thermo-mechanical exfoliation, which is essential to be ascertaining for the technique in an industrial context. The aim of this study concerns the feasibility to reuse the parental Si substrate in the presence of non-planar Si-Al interface originated by the first exfoliation. A numerical method based on the Finite Element Method (FEM) and Linear Elastic Fracture Mechanics (LEFM) is used to simulate the evolution of the non-planar Si-Al interface after successive exfoliations. We find a partial reduction in the amplitude of the transferred groove on the Si-Al interface for grooves having typical realistic dimension. The numerical results are confirmed by the reduction of the amplitude of the groove observed in the experimental tests. These results are promising for the repeated exfoliation from one substrate, inasmuch as the possible roughness on the parental substrate after the first use does not significantly affect the subsequent exfoliations.

© 2016 The Authors. Published by Elsevier Ltd. This is an open access article under the CC BY-NC-ND license (http://creativecommons.org/licenses/by-nc-nd/4.0/).
Peer review by the scientific conference committee of SiliconPV 2016 under responsibility of PSE AG.

*Keywords:*Kerfless wafering; Thermomechanical spallation; Finite element modelling; Fracture mechanics.

* Corresponding author. Tel.: +39 0110905337.
E-mail address: irene.berardone@polito.it

1876-6102 © 2016 The Authors. Published by Elsevier Ltd. This is an open access article under the CC BY-NC-ND license (http://creativecommons.org/licenses/by-nc-nd/4.0/).
Peer review by the scientific conference committee of SiliconPV 2016 under responsibility of PSE AG.
doi:10.1016/j.egypro.2016.07.058

1. Introduction

The theoretical description of spalling can be traced back to the early studies by Suo and Hutchinson [1]. They discovered that cracks in a bi-layered stack, for particular combinations of materials and geometries, may propagate inside the substrate parallel to the bi-layered interface. Their theoretical results have been employed in technological applications to produce thin silicon-based kerf-less layers [2-7].

The analytical model presented in [1] is based on the hypothesis of a two-dimensional semi-infinite plane made of a brittle material with a thin film deposited on the top of it. Residual stresses induced in these components by a uniform temperature variation from a stress-free reference condition are caused by the thermo-elastic mismatch between the two joined materials, here Al and Si.

In the kerf-less experimental and numerical work [6], crack propagation is driven and controlled through a temporally and spatially varying temperature field to achieve a flat exfoliated layer. The multiple use of a substrate wafer in thermally induced spalling has been shown to be feasible by Bellanger et al. [8], using a bi-layer component with notches realized by three laser cuts on its sides. The complex boundary conditions together with the finite size of the samples require the application of a numerical method to simulate crack propagation in realistic conditions [9]. Here, we present the results of the numerical simulations for studying the influence of successive reuses of the Si substrate. The simulated Si-Al stack has just a laser notch on its sides [6]. Experimentally we introduce a groove in a substrate sample and deposit then the Al stressor layer. We compare these samples after exfoliation to examine the effect of a single surface defect and compare it with the simulated results.

2. Numerical approach

We use the finite element analysis program FRacture ANalysis Code (FRANC2D) to simulate the crack path and the required thermal load that has to be imposed to achieve steady-state crack propagation [4]. It allows the computation of the Stress Intensity Factors (SIFs) and the prediction of the conditions for crack propagation of an initial crack depending on the realistic finite geometry and on the specified boundary conditions. The discretization of the continuum is performed by using eight-node isoparametric finite elements. Around the crack tip, quarter-point singular finite elements are used to capture the stress singularity typical of a crack travelling into a homogeneous medium. Automatic mesh refinement at the crack tip is performed during crack propagation in order to avoid the presence of geometrically distorted elements.

Simulation of crack propagation, using this code, requires a sequence of operations. For given boundary conditions and imposed temperature field, which is specified node-wise by a pre-processor developed in MATLAB by the authors, the software FRANC2D solves the linear system of equations resulting from the finite element discretization. For each crack-tip position, the code computes the Mode I and the Mode II SIFs at the crack-tip via the J-integral [10] or via the displacement correlation technique [11] that, for the present study, provide the same numerical results. The computed SIFs are used to predict the crack propagation direction based on three possible fracture criteria: the maximum shear stress criterion [12], the maximum energy release rate criterion [13], and the minimum strain energy density criterion [14]. By comparing the equivalent stress-intensity factor, determined from the SIFs according to one of these criteria, and the material fracture toughness, K_{IC}, the crack propagates if and only if the equivalent stress-intensity factor reaches K_{IC}. Then, a new crack-tip location is determined by imposing a small user-defined crack increment in the suggested crack propagation direction. Subsequently, the code deletes elements along the incremental crack path, updates the crack geometry, and performs automatic local re-meshing. The details on procedures for crack propagation and re-meshing schemes are described in [15].

For this analysis we use the J-integral algorithm for the computation of the stress-intensity factors and the minimum strain energy density as the criterion to determine the crack growth direction, as in [9]. Thus, the crack propagates in the direction where the strain energy density is minimum. We apply a thermal load of $\Delta T = -43K$, which is the temperature difference with respect to the stress-free temperature. The material parameters of the analysed system are: Young's modulus (E), Poisson's ratio (ν), coefficient of thermal expansion (CTE) and critical

stress-intensity factor (K_{IC}). In our simulations we use the following parameters for silicon and aluminum summarized in Table 1.

Table 1. Material parameters used in the simulations.

Material parameters	Silicon	Aluminum
E	139 GPa	68 GPa
K_{IC}	0.75 MPa $m^{0.5}$	24 MPa $m^{0.5}$
ν	0.276	0.34
CTE	$0.26x10^{-5}$ °C^{-1}	2.3 $x10^{-5}$ °C^{-1}

The geometrical parameters are illustrated in Fig.1a.The amplitude of the groove in the y-direction is set to *b*=20 µm, which is an extreme value used in the benchmark experimental tests, to evaluate a worst-case scenario after the first exfoliation. Different lengths of the groove, *L*, in the x-direction are considered, i.e., *L*= 125, 250, 500, 800 and 1000 µm. From the semi-analytic model in [5], we expect at steady state a crack depth λh=77.50 µm far from the groove, and λh=96.25 µm below the groove. The mean value of the height of the Si-substrate after the crack propagation (λ_0h - λh) at the equilibrium in the region that follows the groove and in the region under the groove are displaced in Fig, 1 (b). From the numerical results, we find that in the region following the groove the parental Si-substrate is not influenced by the previous zone for all the value of *L* considered, in contrast to the region under the groove.

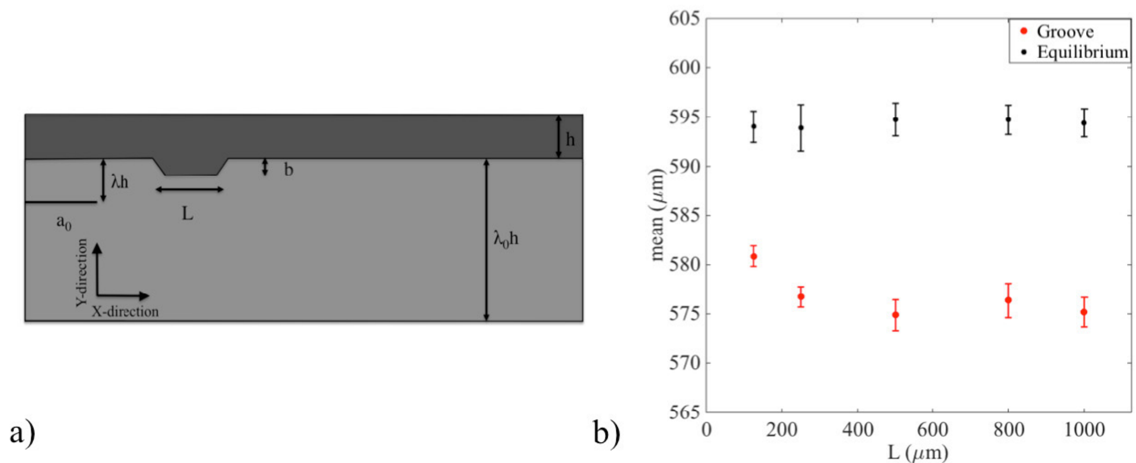

Fig.1 a) Geometry of the sample with the initial groove. The span of the specimen is 14 cm, the thickness of the silicon substrate is λ_0h=675 µm, the thickness of the aluminium is h=125 µm, the initial crack depth is λh=83 µm, the initial notch size is a_0=190 µm, the height of the groove is b=20 µm, the width of the groove is L. b) Mean value of the height of the silicon-substrate after the crack propagation (λ_0h-λh) at the equilibrium in the region that follows the groove and in the region under the groove, where the error bars are given by the relative errors respect to the initial crack position.

The sketch of the non-planar interface, for the considered values of L, is shown in the upper part of Fig. 2 and the crack path during crack propagation in the silicon substrate is shown in the bottom part. The y-axis displaces the Si-Al interface and the crack path using the axis convention shown in Fig. 1(a). From the results shown in Fig. 2 we

find that the amplitude of the discontinuity transferred to the Si substrate after the exfoliation in the y-direction (b') remains in the same order of magnitude as the depth of the groove b = 20 µm before the first exfoliation.

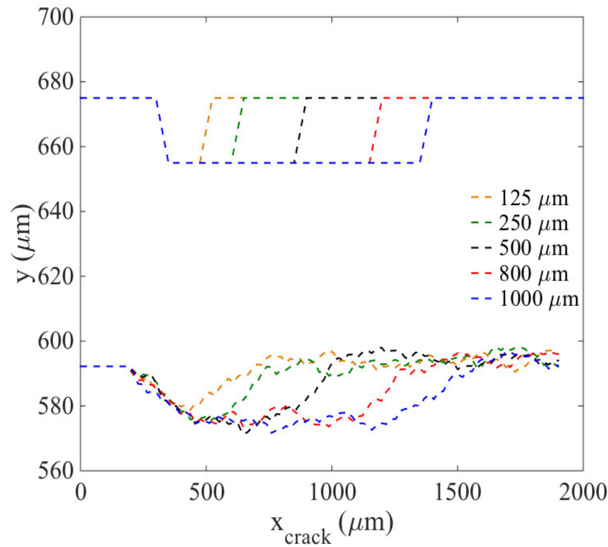

Fig. 2. On the top: sketch of the geometry of the initial groove along the silicon-aluminium interface. On the bottom: simulated crack path in the Si-substrate showing the change of the groove shape after reuse.

However, for L<250 µm, a reduction of b' is noticed, see Fig. 3. Thus, numerical results suggest a better feasibility of reusing Si substrates provided that the non-planarity of their surface after the first exfoliation has proper geometrical features, i.e., the extension of the groove is less than 250 µm.

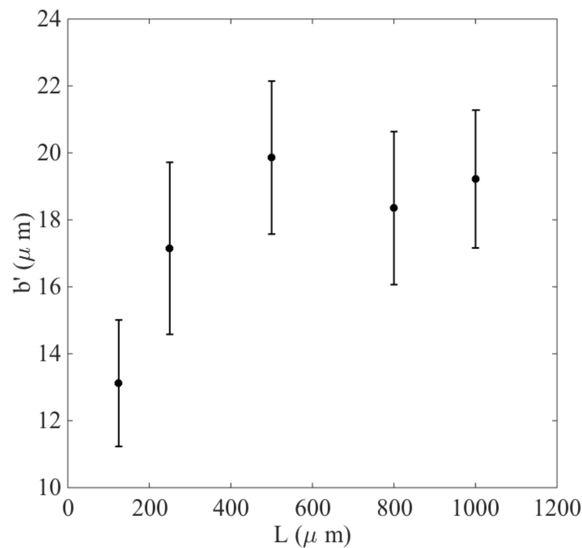

Fig. 3 Amplitude of the groove transferred on the substrate after crack propagation.

We evaluate the resulting width of the transferred groove (L') after spalling. To overcome the fluctuations due to the numerical error in the y-direction, we set a threshold value in the y-direction defined as a percentage of 99.2% of the minimum value achieved.

Fig. 4 shows in black the transferred width of the groove (*L*') after spalling vs. the width of the original one (*L*). The error is defined as the sum of the numerical uncertainly in the *x*-direction and the threshold error. Considering y_t the threshold and y_m the average value in the region *L*', the latter contribution to the error is defined as x_t-x_m, where x_t is the region with $y \leq y_t$ and x_m is the region where $y \leq y_m$. The red dashed line represents the condition in which the transferred groove has the same dimension of the original one (*L*'=*L*). The dimension of the transferred base of the groove is generally reduced compared to the original one (see the red dashed line)

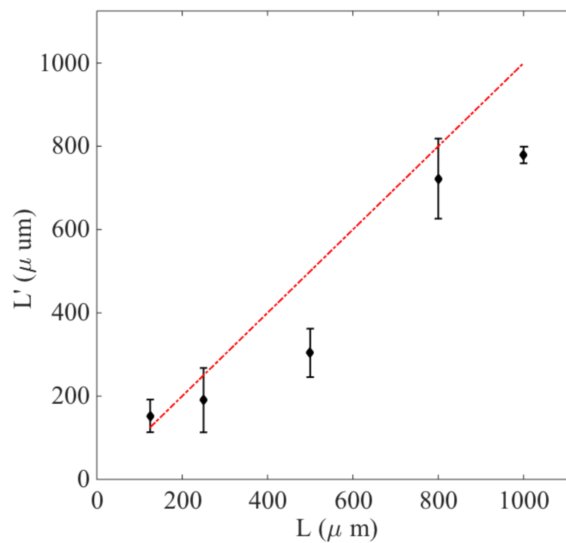

Fig.4. Width of the groove after the exfoliation L' vs. original width L. The black dots are the simulated width of the groove after spalling with their error-bar and the red dashed line represents the condition in which the transferred groove has the same dimension of the original one (*L*'=*L*).

Moreover we compare the cross-section area C_A (see Fig.5 (a)) of the groove transferred to the parental substrate after the exfoliation with the initial groove (Fig.5 (b)). Black dots are the cross-section areas obtained from the simulation, while the red dashed line is the linear fit. Thus, numerical results show that the cross-section area of the groove after the exfoliation increases linearly with the size of the initial width of the groove.

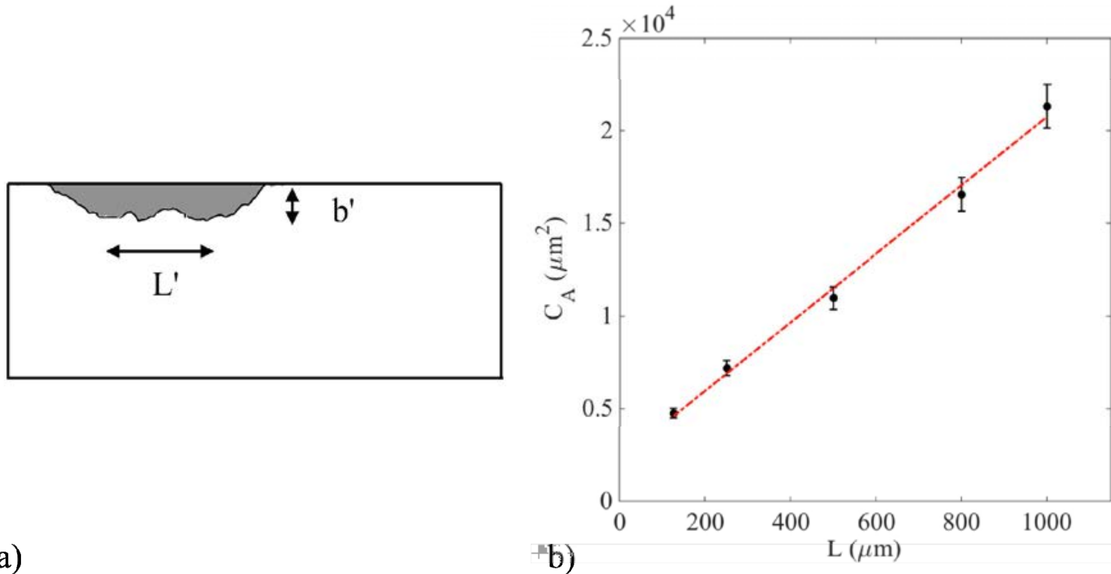

Fig.5. a) Sketch of the removed cross-section area C_A (grey region) inside the parental substrate after the exfoliation with respect to the flat surface due to the presence of the groove, with height *b'* and width *L'* transferred to the substrate. b) Resulting cross-section area C_A (black dots) vs. width *L* of the groove. The red dashed line is the linear fit of the resulting data.

3. Experiment and results

Fig. 6 (a) shows an optical microscope cross-section of a Si and Al bi-layer system with initial groove. The V-shaped groove has been created in Si with a dicing saw and a wet chemical etching in order to remove surface defects. We use 50% of KOH at a temperature of 90°C for 2 min. The etch rate of KOH is strongly affected by the crystallographic orientation of Si (anisotropic). Afterwards, Al is evaporated on top of the Si wafer. The resulting bi-layer system is characterized by the following groove parameters: L=22.66 µm, b=17.25 µm. The cross-section of the parental silicon substrate after exfoliation by optical microscope measurement is shown in Fig. 6 (b), where the black arrow indicates the centre of the initial groove.

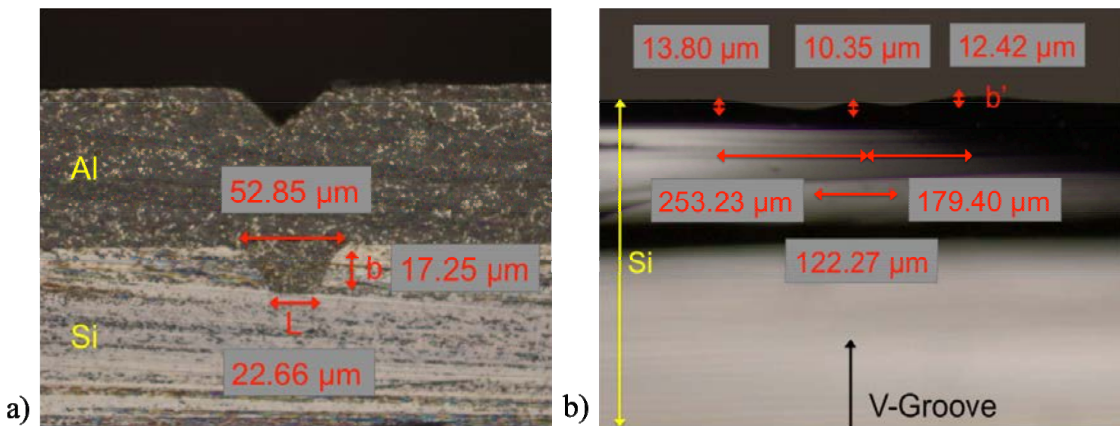

Fig. 6. a) Optical microscope cross-section of Si and Al bi-layer system with initial groove. b) Optical microscope measurement of a cross-section of the Si parental substrate after exfoliation.

The height of the groove transferred on the substrate *b'* is reduced of the 24% compared to the initial *b* after reuse, as it can be seen from Fig. 6 (b). Indeed, the average value of measurements of the transferred groove to the Si substrate after the exfoliation in the y-direction (b') is reduced to 13.11 μm. The particular shape of the rough region is the result of dynamic effects occurring during crack propagation that were not considered in the numerical simulations.

We look into details on delaminated edge surface resulting from the standard spalling process, i.e. without V-groove. We crarry out this further analysis for two reason. The first is that at the edge the difference in the heights is maximum, either due to the non ideal alignment of the laser cut or due to the initial unsteady crack propagation regime. The second is the corresponance between the analyzed region and the next crack iniziation position.

The surface measurement is carried out with a Leica DCM-3D contactless confocal profilometer in the laboratory of the Research Unit Multi-scaleAnalysis of Materials (MUSAM) of the IMT School for Advanced Studies Lucca. Fig. 7 shows the 3D topography of a part of the surface with the dimensions 5000 x 1500 μm^2, taken from a whole sample having a size of 5000 x 50000 μm^2. Five profile lines, characterizing the crack trend in different directions, are identified: lines from 1 to 3 are parallel to the *y*-direction, in particular the first is near the edge (x = 500 μm), the second is in the first half of the sample (x = 1500 μm) and the third one is in the middle of the sample (x = 2500 μm). The line number 4 crosses the entire sample along the *x*-direction starting from y = 750 μm. The last line, number 5, is oblique for catching only the fluctation and it meets the border of the sample. In the bottom part of Fig. 7, from (b) – (d), the profilometric scans of the 5 described lines are shown. These are normalized with respect to the minimum height of the profile. Graph 7 (b) shows the profile of the lines parallel to the *y*-direction. In particular, the line No. 1, the nearest to the edge, shows oscillation around its average value of 1.58 with a variance of 0.11. In this region the crack has not reached the quasi-steady propagation condition and the fluctuations are due to that. The profile of line no. 2 shows a trend with very small fluctuations. Finally the profile of line no.3 shows a rather smooth trend until the steady state conditions are met along the *y*-direction. Herein the average is 1.69 μm and the variance 0.03 μm. The second chart instead shows profile line no.4 which shows that the central part of the sample is quite flat and the oscillations are almost all localized at the edges, conferming what was already found in [16], with an average elevation of 1.33 respect to the minimum. The variation along the line no.4 at the center is probably due to a difference in the laser allignment between the two sides.

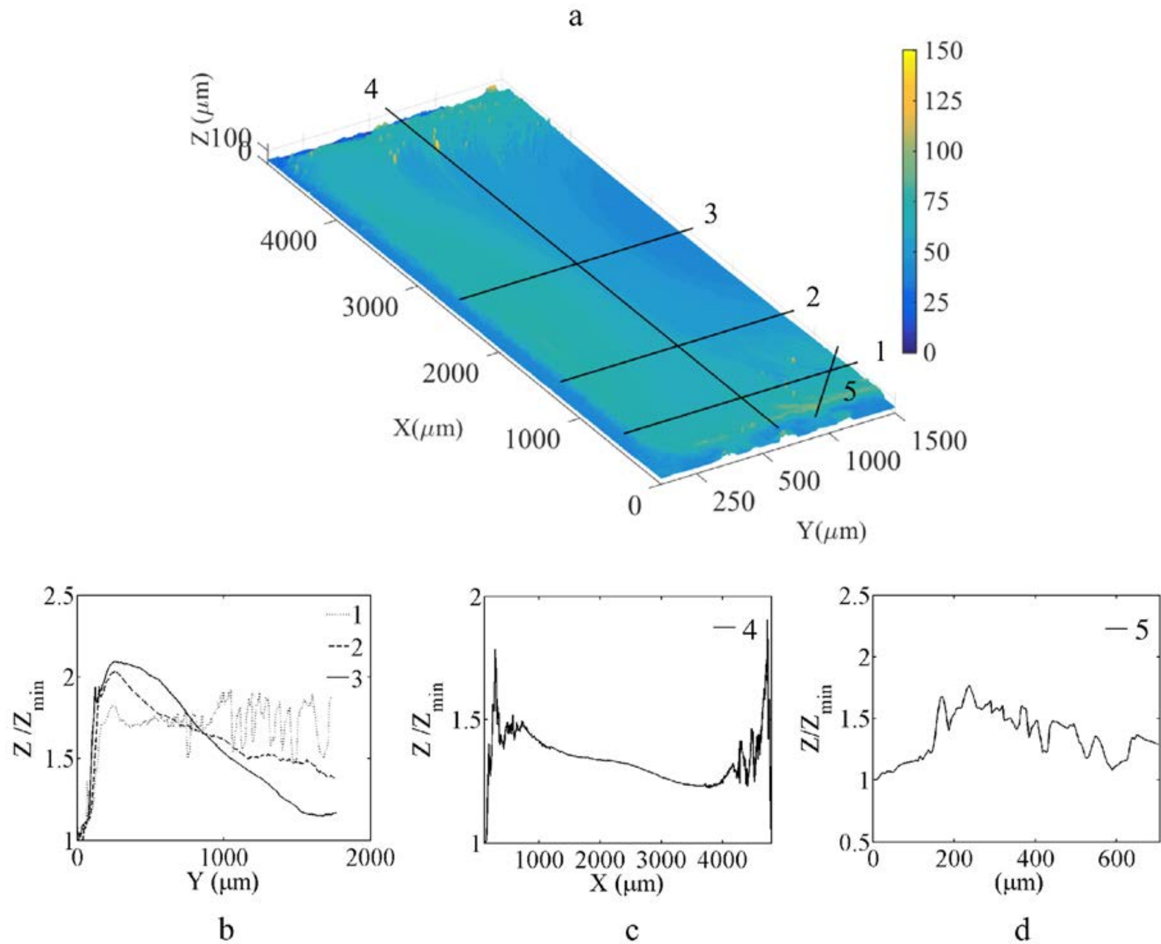

Fig. 7. Top part: (a) the surface the initial region (5x1.5 mm) of a sample, with a whole dimension of 5x50 mm, where 5 significant lines are identified. Bottom part: (b) Lines 1-3 are parallel to the *y*-direction. (c) The line crosses the entire sample along the *x*-direction. (d) The last line is oblique and it matches the border of the sample.

4. Conclusion

According to a numerical method based on the finite element method and linear elastic fracture mechanics, a partial reduction in the amplitude of the initial groove has been predicted, in particular for low values of the groove width. Numerical predictions are confirmed by experimental tests on artificially created V-grooves in silicon substrates. A further study on the edge of a delaminated surface without an initial artificial groove has been conducted. The roughness measurements of the edge of the delaminated surface show an extremely flat central region, with edge roughness caused by the laser cut and by the transient heat-transfer heat conduction during the fast cooling process during spalling. These results are encouraging for the reuse of silicon wafers because it has been shown that the depth of the grooves does not increase after a first spalling, which ensures the feasibility of the production process.

Acknowledgements

MP would like to acknowledge funding from the European Research Council under the European Union's Seventh Framework Programme (FP/2007-2013) / ERC Grant Agreement n. 306622 (ERC Starting Grant "Multi-field and multi-scale Computational Approach to Design and Durability of PhotoVoltaic Modules"–CA2PVM). IB acknowledges the support of DAAD (German Academic Exchange Service) with the short term grant. This work was also supported by the Federal Ministry for Environment, Nature Conservation, and Nuclear Safety under the contract FKZ 0325461 and by the state of Lower Saxony, Germany. The authors would like to acknowledge Dr. Claudia Borri at the IMT School for Advanced Studies Lucca for profilometric measurements.

References

[1] Suo Z, Hutchinson JW. Steady-state cracking in brittle substrates beneath adherent films. Int J Solids Struct 1989;25:1337-53.
[2] Rao RA, Mathew L, Saha S, Smith S, Sarkar D, Garcia R, Stout R, Gurmu A, Ahn D, Xu D, Jawarani D, Onyegam E, Hilali M, Banerjee S, Fossum J. A novel low-cost 25 μm thin exfoliated monocrystalline Si solar cell technology. Procedings of 26th European Photovoltaic Energy Conference, Hamburg, Germany 2011. p. 2439-42.
[3] Dross F, Robbelein J, Vandevelde B, Van Kerschaver E, Gordon I, Beaucarne G, Poortmans J. Stress-induced large-area lift-off of crystalline Si films. Appl Phys A Mater 2007;89:149-52.
[4] Martini R, Gonzalez M, Dross F, Masolin A, Vaes J, Frederickx D, Poortmans J. Epoxy-induced spalling of Silicon. Energy Procedia 2012;27:567-72.
[5] Bellanger P, Brito MC, Pera MD, Costa I, Gaspar G, Martini R, Debucquoy M, Serra JM. New stress activation method for kerfless Silicon wafering using Ag/Al and Epoxy stress-inducing layers. IEEE J Photovolt 2014;5:1228-34.
[6] Hensen J, Niepelt R, Kajari-Schröder S, Brendel R. Directional heating and cooling for controlled spalling. IEEE J Photovolt 2015;1:195-01.
[7] Tanielian M, Blackstone S, Lajos RS. New technique of forming thin free standing single-crystal films. J Electrochem Soc 1985;132:507-09.
[8] Bellanger P, Sousa P, Bouchard PO, Bernacki M, Brito MC, Serra JM. Room temperature spalling of silicon thin foils using a stress inducing epoxy layer. Procedings of the 29th European Photovoltaic Solar Energy Conference and Exhibition, Amsterdam, Netherlands; 2014 p. 579-82.
[9] Berardone I, Kajari-Schröder S, Niepelt R, Hensen J, Steckenreiter V, Paggi M. Numerical modelling and validation of thermally-induced spalling. Energy Procedia 2015;77:855-62.
[10] Rice JR. A path independent integral and the approximate analysis of strain concentration by notches and cracks. J Appl Mech 1968;35:379-86.
[11] Raju IS. Calculation of strain-energy release rates with higher order and singular finite elements. Eng Fract Mech 1987;28:251-74.
[12] Tracey MD. Finite elements for determination of crack tip elastic stress intensity Factors. Eng Fract Mech 1971;3:255-65.
[13] Erdogan F, Sih GC. On the crack extension in plates under plane loading and transverse shear. J Basic Eng-T ASME 1963;4:519-25.
[14] Hussain MA, Pu SL, Underwood J. Strain energy release rate for a crack under combined mode I and mode II. Fracture Analysis, ASTM STP 1993;2:28.
[15] Sih CG. Strain-energy-density factor applied to mixed mode crack problems. International Journal of Fracture 1974;305:21-10.
[16] Niepelt R, Hensen J, Knorr A, Steckenreiter V, Kajari-Schöder S, Brendel R. High-quality exfoliated crystalline silicon foils for solar cell applications. Energy Procedia 2014;55:570-77.